

Papers published in *Ocean Science Discussions* are under open-access review for the journal *Ocean Science*

Tidal modulation of two-layer hydraulic exchange flows

L. M. Frankcombe^{1,*} and A. McC. Hogg¹

¹Research School of Earth Sciences, The Australian National University, Canberra, Australia
*now at: Institute for Marine and Atmosphere Research Utrecht, Department of Physics and Astronomy, Utrecht University, The Netherlands

Received: 1 November 2006 – Accepted: 20 November 2006 – Published: 27 November 2006

Correspondence to: L. M. Frankcombe (l.frankcombe@phys.uu.nl)

OSD

3, 1999–2020, 2006

Tides in exchange flows

L. M. Frankcombe and
A. McC. Hogg

Title Page

Abstract

Introduction

Conclusions

References

Tables

Figures

⏪

⏩

◀

▶

Back

Close

Full Screen / Esc

Printer-friendly Version

Interactive Discussion

EGU

Abstract

Time-dependent, two layer hydraulic exchange flow is studied using an idealised shallow water model. It is found that barotropic time-dependent perturbations, representing tidal forcing, increase the baroclinic exchange flux above the steady hydraulic limit, with flux increasing monotonically with tidal amplitude (measured either by height or flux amplitude over a tidal period). Exchange flux also depends on the non-dimensional tidal period, γ , which was introduced by Helfrich (1995). Resonance complicates the relationship between exchange flux and height amplitude, but, when tidal strength is characterised by flux amplitude, exchange flux is a monotonic function of γ .

1 Introduction

Flow of stratified water through ocean straits makes an important contribution to the evolution of ocean stratification, affecting global circulation and the local dynamics of estuaries and semi-enclosed basins. For example, exchange flow through the Strait of Gibraltar at the mouth of the Mediterranean Sea controls the salinity budget of the evaporative Mediterranean basin (Bray et al., 1995). Furthermore, the dense, saline outflow of water from Gibraltar can be detected as a distinct water mass across the North Atlantic (Sy, 1988; Harvey and Arhan, 1988). It follows that characterisation of flow through straits is an important problem, especially considering the difficulty most ocean and climate models face in resolving strait dynamics.

Internal hydraulic theory can give a useful estimate of density-driven flow through straits in particular cases (Wood, 1970; Armi, 1986). This theory can be used to predict an upper bound for exchange flow through a strait (Armi and Farmer, 1987). However, this upper bound can be exceeded in cases where a time-dependent forcing, such as tidal flow, exists (Armi and Farmer, 1986).

Stigebrandt (1977) proposed a simple amendment to the hydraulic solution which showed reasonable agreement with laboratory experiments. This theory was super-

OSD

3, 1999–2020, 2006

Tides in exchange flows

L. M. Frankcombe and
A. McC. Hogg

Title Page

Abstract

Introduction

Conclusions

References

Tables

Figures

◀

▶

◀

▶

Back

Close

Full Screen / Esc

Printer-friendly Version

Interactive Discussion

EGU

seded by [Armi and Farmer \(1986\)](#), who formulated a quasi-steady solution based on hydraulically controlled solutions with a barotropic throughflow. The quasi-steady solution assumed that tidal variations were sufficiently slow so that hydraulic control was continually established; however, hydraulic control itself is not well defined in a time dependent flow and it can be shown that tidal variations may exceed the frequency over which the quasi-steady solution is valid. [Helfrich \(1995\)](#) introduced a nondimensional parameter, γ , the ratio of tidal period to the time taken for a wave to traverse the strait. It is defined as

$$\gamma \equiv \frac{T \sqrt{g'H}}{l} \quad (1)$$

where T is the period of the wave, $g' = g\Delta\rho/\rho$ is reduced gravity, H is the total fluid height and l is the length scale of the channel, i.e. the distance between the narrowest part of the channel (where channel width is b_0) and the point where channel width is $2b_0$. [Helfrich \(1995\)](#) predicted that flux would depend upon both the dynamic strait length γ , and the amplitude of the tide. This prediction was consistent with simulations from a simple numerical model with a rigid lid. [Helfrich](#) also conducted laboratory experiments which showed that flux depends on γ , but that mixing and other effects act to reduce the flux.

Additional experiments were conducted by [Phu \(2001\)](#) (reported by [Ivey, 2004](#)), in which both tidal amplitude and frequency were varied. It was found that exchange flux was strongly dependent on tidal amplitude, but that there was no systematic dependence upon tidal period, over a wide range of $2 < \gamma < 70$ ([Ivey, 2004](#)). This finding is inconsistent with the analytical predictions, numerical simulations and experiments of [Helfrich \(1995\)](#).

In this paper we take a different, numerical, approach with the goal of establishing the role of tidal period in exchange flows. We use a simple two-layer model of the shallow water equations to calculate the response of hydraulic exchange flows to time-dependent forcing. Barotropic forcing is induced at the boundaries and propagates into the domain as a free surface wave (unlike [Helfrich's](#) baroclinic numerical model which

Tides in exchange flows

L. M. Frankcombe and
A. McC. Hogg

[Title Page](#)[Abstract](#)[Introduction](#)[Conclusions](#)[References](#)[Tables](#)[Figures](#)[◀](#)[▶](#)[◀](#)[▶](#)[Back](#)[Close](#)[Full Screen / Esc](#)[Printer-friendly Version](#)[Interactive Discussion](#)

used a rigid lid). The waves modify the flux, which can be accurately measured, and the results are compared to the quasi-steady solution of [Armi and Farmer \(1986\)](#), the predictions of [Helfrich \(1995\)](#) and the experimental results of [Phu \(2001\)](#).

We begin the paper by outlining the model and boundary conditions in Sect. 2. Section 3 shows the results of the model, which are developed to span a wide parameter space in both the frequency and amplitude of time-dependent forcing. These results are discussed in Sect. 4, and application to geophysical flows is considered.

2 The Model

2.1 Shallow water equations

The model used here is formulated to include the physics of time-dependent exchange flows with the minimum possible alterations to the steady hydraulic equations. We therefore solve the one-dimensional nonlinear shallow water equations for flow along a rectangular channel. The channel has length $2L$ and variable width $b(x)$. We assume that flow occurs within two distinct immiscible fluid layers. The thickness of each layer is $h_i(x, t)$ – as shown in Fig. 1. The layers are assumed to have constant density ρ_i , and velocity $u_i(x, t)$ which depends upon horizontal, but not vertical, position.

The conservation of mass (or continuity) equation for each layer is given by

$$\frac{\partial h_i}{\partial t} = -\frac{1}{b} \frac{\partial}{\partial x} (bu_i h_i). \quad (2)$$

The conservation of momentum equations are

$$\frac{\partial u_1}{\partial t} + u_1 \frac{\partial u_1}{\partial x} = -g \frac{\partial}{\partial x} (h_2 + h_1) + g' \frac{\partial h_2}{\partial x} + A_h \frac{\partial^2 u_1}{\partial x^2} \quad (3)$$

and

$$\frac{\partial u_2}{\partial t} + u_2 \frac{\partial u_2}{\partial x} = -g \frac{\partial}{\partial x} (h_2 + h_1) + A_h \frac{\partial^2 u_2}{\partial x^2}, \quad (4)$$

Tides in exchange flows

L. M. Frankcombe and
A. McC. Hogg

Title Page

Abstract

Introduction

Conclusions

References

Tables

Figures

◀

▶

◀

▶

Back

Close

Full Screen / Esc

Printer-friendly Version

Interactive Discussion

where the reduced gravity, g' , is defined as follows:

$$g' \equiv \frac{g(\rho_1 - \rho_2)}{\rho_1}.$$

Note that we have included a lateral viscosity with a constant coefficient A_h , which is required for numerical stability but is minimised in the simulations.

The solution of (2)–(4) under the assumption of a steady flow may yield hydraulically controlled flow solutions (depending upon the boundary conditions at either end of the channel). The full time-dependent equations may be solved numerically in a straightforward manner; but results are again dependent upon the correct boundary conditions.

2.2 Boundary conditions

The boundary conditions used for this model are the characteristic open boundary conditions based on the time-integrating conditions proposed by Nycander and Döös (2003) and further developed for inertial flows by Nycander et al. (2006). These conditions require us to specify characteristic variables a_E^\pm and a_I^\pm at each of the open boundaries. The variables are defined as

$$a_E^\pm = \frac{1}{2H} \left[h_1 + h_2 \pm \frac{H_1 u_1 + H_2 u_2}{\sqrt{gH}} \right], \quad (5)$$

$$a_I^\pm = \frac{1}{2H} \left[\frac{H_1 h_2 - H_2 h_1}{H} \pm \sqrt{\frac{H_1 H_2}{g'H - \Delta U^2}} (u_2 - u_1) \right]. \quad (6)$$

These equations are formulated by linearising the equations about a state with layer heights H_1 and H_2 (where $H=H_1 + H_2$), and velocity difference ΔU between the layers.

Tides in exchange flows

L. M. Frankcombe and
A. McC. Hogg

Title Page

Abstract

Introduction

Conclusions

References

Tables

Figures

◀

▶

◀

▶

Back

Close

Full Screen / Esc

Printer-friendly Version

Interactive Discussion

The conditions are implemented as follows. Assume, for example, that the boundary is an h -point of a staggered grid. Then we must specify the inward travelling characteristic variables a_E^\pm and a_I^\pm . Having done that, the values of h_1 and h_2 at the boundary can be expressed in terms of a_E^\pm , a_I^\pm and the values of u_1 and u_2 at the point just inside:

$$5 \quad h_1(\mp L) = 2H_1 a_E^\pm - 2H_1 a_I^\pm \mp \frac{H_1}{H} \frac{H_1 u_1 + H_2 u_2}{\sqrt{gH}} \pm \sqrt{\frac{H_1 H_2}{g'H - \Delta U^2}} (u_1 - u_2), \quad (7)$$

$$h_2(\mp L) = 2H_2 a_E^\pm + 2H_2 a_I^\pm \mp \frac{H_2}{H} \frac{H_1 u_1 + H_2 u_2}{\sqrt{gH}} \mp \sqrt{\frac{H_1 H_2}{g'H - \Delta U^2}} (u_1 - u_2). \quad (8)$$

10 The above conditions are suitable for sub-critical flow, but this model also needs to be able to simulate supercritical two-layer flow. The model is designed to switch to supercritical flow boundary conditions subject to a test on the criticality of the flow. There are two modes of supercritical flow (i.e. supercritical with respect to barotropic and baroclinic modes) and therefore two tests. The test for supercritical barotropic flow
15 is based on the linear phase speed of a barotropic wave. When

$$\frac{h_1 u_1 + h_2 u_2}{h_1 + h_2} > \sqrt{g(h_1 + h_2)}, \quad (9)$$

at the right hand end of the channel, flow is adjudged supercritical. There is an analogous condition at the left hand end of the channel. When this test is satisfied, the supercritical open boundary conditions are simply

$$20 \quad \frac{\partial h_1}{\partial x} = \frac{\partial h_2}{\partial x} = 0, \quad (10)$$

Tides in exchange flows

L. M. Frankcombe and
A. McC. Hogg

Title Page

Abstract

Introduction

Conclusions

References

Tables

Figures

◀

▶

◀

▶

Back

Close

Full Screen / Esc

Printer-friendly Version

Interactive Discussion

which replaces (7)-(8).

Internally supercritical flow is more complicated. Firstly, using linear internal wavespeeds to test for internal criticality, we obtain

$$\frac{h_2 u_1 + h_1 u_2}{h_1 + h_2} > \sqrt{\frac{h_1 h_2}{(h_1 + h_2)^2} (g'(h_1 + h_2) - (u_1 - u_2)^2)}, \quad (11)$$

5 at the right hand end of the channel (and an analogous condition for the left hand end). It should be noted that the RHS of this condition becomes imaginary when shear is strong, in which case the wavespeeds coalesce and waves are unstable. Therefore, we propose that a suitable test for criticality is simply

$$\frac{h_2 u_1 + h_1 u_2}{h_1 + h_2} > \sqrt{\frac{h_1 h_2}{(h_1 + h_2)^2}} \Theta, \quad (12)$$

10 where

$$\Theta \equiv \max \left(0, \left(g'(h_1 + h_2) - (u_1 - u_2)^2 \right) \right). \quad (13)$$

The boundary conditions for internally supercritical flow are found by assuming that the internal mode is captured primarily by interfacial height, and so we set

$$\frac{\partial h_1}{\partial x} = 0, \quad (14)$$

15 with h_2 calculated using the addition of (7) and (8).

2.3 Numerical implementation

The domain is spatially discretised on a staggered grid. Velocity is calculated at the faces of the cells, while layer height is calculated at the centre of the cell. The equations may then be integrated in time using centred differences. The staggered grid is defined so that the near-boundary values of velocity can be explicitly calculated from (3,4).

20

Tides in exchange flows

L. M. Frankcombe and
A. McC. Hogg

Title Page

Abstract

Introduction

Conclusions

References

Tables

Figures

◀

▶

◀

▶

Back

Close

Full Screen / Esc

Printer-friendly Version

Interactive Discussion

The temporal discretisation employs a leapfrog timestep scheme. Leapfrog timestepping routines can produce two diverging solutions. To eliminate this potential problem, data from different time levels are mixed every 1000 timesteps. The standard parameter set for the simulations is shown in Table 1.

3 Results

3.1 Exchange flows

The model is initialised with two constant depth, zero velocity layers. Layer depth variations and velocity are induced by specifying the characteristic boundary conditions, as seen in the series of snapshots in Fig. 2, which shows the development of the exchange flow. Internal waves propagate from either side of the domain, reaching the centre of the constriction after about 1 s. Over the next second, hydraulic control is established at the centre of the channel, and features resembling hydraulic jumps are formed. It should be noted that the model equations used here cannot resolve shocks of this nature, and these jump-like features are only stabilised with viscosity. These features propagate out of the domain, leaving a final steady state exactly matching the two-layer maximal hydraulic exchange flow solution, in which flow is internally supercritical at both ends of the channel. It is notable that there are no significant reflections from the characteristic open boundary conditions during this adjustment process – this issue is examined more closely by [Nycander et al. \(2006\)](#).

Time dependence is introduced to this flow by sinusoidally varying the left boundary condition coefficient, a_e^+ , with a period of 0.5 s. This simulates a barotropic wave entering from the left, as seen in Fig. 3. The incoming wave travels towards the centre of the channel where it interacts with the contraction, causing reflections (both baroclinic and barotropic) to travel back to the left, while the original barotropic wave, which now includes a small baroclinic component, continues to the right. The waves steepen due to nonlinearity as they propagate along the channel.

Tides in exchange flows

L. M. Frankcombe and
A. McC. Hogg

Title Page

Abstract

Introduction

Conclusions

References

Tables

Figures

◀

▶

◀

▶

Back

Close

Full Screen / Esc

Printer-friendly Version

Interactive Discussion

Barotropic flux as a function of time at the left-hand boundary is shown in Fig. 4. Note that the system takes several periods for the oscillations to become regular, as instantaneous flux is modulated by waves reflected off the contraction. For this reason all results in the following sections were calculated after the initial adjustment had occurred.

3.2 Exchange flux in time-dependent systems

The quantity of primary interest in these simulations is the flux of volume (or mass) exchanged. We quantify this by calculating the total flux in each layer as a function of time, integrating over a tidal period and averaging the (absolute value of the) two layer fluxes. This baroclinic exchange flux is then proportional to the net exchange of mass (or passive tracer) through the channel. Figure 5 shows the exchange flux anomaly as a function of nondimensional period γ , for several cases. The flux anomaly has been scaled by the quasi-steady flux, which was calculated numerically from a series of steady simulations and sets a theoretical upper limit for the flux.

In the small period (small γ) limit the flux anomaly approaches zero (the steady hydraulic limit), and in the large γ limit it approaches the quasi-steady solution in each of the three cases shown. This is consistent with the predictions of Helfrich (1995); however here the flux is not a monotonically increasing function of γ . Instead, there are additional local maxima (the largest being at $\gamma \approx 3$) which sometimes exceed the quasi-steady limit. These discrepancies are greatest when g' is large, and when the domain length L is increased (dashed line in Fig. 5).

These peaks are due to resonance in the channel between the open boundary and the contraction. Although the resonance is damped it is continually forced by incoming energy, and thus has a bounded amplitude. Resonance is strongest when the channel is long (allowing time for nonlinear steepening to occur), and can be minimised using small g' (possibly because interactions between barotropic and baroclinic modes are minimised in this case). The resonant period depends on the channel length L as expected. This resonance occurs even though reflections caused by the boundary

Tides in exchange flows

L. M. Frankcombe and
A. McC. Hogg

Title Page

Abstract

Introduction

Conclusions

References

Tables

Figures

◀

▶

◀

▶

Back

Close

Full Screen / Esc

Printer-friendly Version

Interactive Discussion

conditions are significantly smaller than other schemes (Nycander et al., 2006), so it follows that simulations with other boundary conditions, or lab experiments with solid end walls, will experience greater problems with resonance. We do not investigate the source of resonance in this paper; instead, for all tests below, the simulations use $L=0.5$ and $g'=0.1$ to minimise the effect. We use these simulations to quantify the effect of tidal period and amplitude on exchange flux.

3.3 Rescaling amplitude

Although resonance is minimised through choice of parameters, it cannot be entirely eliminated. Notably, this resonance was not observed in Helfrich's (1995) simulations (which used a rigid upper surface and imposed barotropic fluctuations at the contraction). For consistency with previous work, we prefer to further reduce resonant effects by taking the observed amplitude of the waves at the centre of the channel (instead of the amplitude originally imposed at the boundary). It is then possible to define two tidal amplitudes. Firstly, a represents the peak-to-trough amplitude of fluid height over the tidal cycle. We refer to this as the **height amplitude** and it is analogous to the method used by Phu (2001) to characterise tidal amplitude. Secondly we can use the barotropic **flux amplitude**, Helfrich's q_{b0} parameter, which is defined as

$$q_{b0} \equiv \frac{u_{b0}}{\sqrt{g'H}} \quad (15)$$

where u_{b0} is the peak-to-trough amplitude of barotropic velocity at the throat over the tidal cycle.

This allows us to plot measured (a) height and (b) flux amplitude against γ , as in Fig. 6 (note the logarithmic axes). Here we see the effect of the resonance – the measured amplitude, for a given value of imposed a_e^+ amplitude, is not independent of γ . Moreover, the two measures of amplitude differ significantly as a function of γ .

Numerous simulations across a large range in γ and a_e^+ amplitude were conducted and the results have been interpolated onto lines of (a) constant height amplitude, and

Tides in exchange flows

L. M. Frankcombe and
A. McC. Hogg

Title Page

Abstract

Introduction

Conclusions

References

Tables

Figures

◀

▶

◀

▶

Back

Close

Full Screen / Esc

Printer-friendly Version

Interactive Discussion

Tides in exchange flowsL. M. Frankcombe and
A. McC. Hogg

[Title Page](#)[Abstract](#)[Introduction](#)[Conclusions](#)[References](#)[Tables](#)[Figures](#)[⏪](#)[⏩](#)[◀](#)[▶](#)[Back](#)[Close](#)[Full Screen / Esc](#)[Printer-friendly Version](#)[Interactive Discussion](#)

(b) constant flux amplitude. We can now plot flux as a function of γ for a number of different cases – see Fig. 7. Figure 7a shows a peak at $\gamma=1.5$, indicating that height amplitude is not a good measure of the tidal effect on exchange flows. It follows that for cases with greater amplitude and stronger stratification, such as the dashed lines in Fig. 5, the height amplitude will be a very poor descriptor of the tidal effects. Figure 7b, on the other hand, clearly shows a smooth monotonic transition of flux with γ when flux amplitude is used as the metric. These results are consistent with predictions of Helfrich (1995). Thus flux amplitude would appear to be a more useful metric than height amplitude.

The results are re-plotted in Fig. 8, showing amplitude vs flux for each of the above cases. The panels, showing scaled flux as a function of height and flux amplitude respectively, both show a clear tendency for flux to increase with amplitude. This is consistent with expectations and with results of Phu (2001). The differences between the height and flux amplitude are once again noticeable, however the overall trend remains the same in both cases.

4 Discussion and conclusions

The results of these simulations confirm that time-dependent forcing leads to an increase in exchange flux compared to the steady state case. Tidal amplitude, as measured by either height or flux amplitude, has a strong effect on flux, with flux increasing monotonically with amplitude.

Flux also depends on the nondimensional tidal period γ . However, resonance with the open boundary conditions in the numerical simulations performed here modulates the response. Resonance produces effects which depend strongly upon tidal period. Nevertheless, if one uses the flux amplitude to characterise tidal strength, then the exchange flux is a monotonic function of γ . The relationship between exchange flux and height amplitude, on the other hand, is more complicated. Depending on the strength of resonance this may result in a non-monotonic relationship between exchange flux

and γ (when a is held constant).

These observations may explain some outstanding discrepancies between previous studies on this topic. [Phu \(2001\)](#) (reported by [Ivey, 2004](#)) used the height amplitude to characterise tidal strength and found no systematic dependence upon γ over a wide range in parameter space, while [Helfrich \(1995\)](#) found a strong dependence of flux amplitude on γ . Reflections from the solid tank walls in [Phu's \(2001\)](#) experiments would have produced resonance, especially for large values of γ (long periods) where there is ample time for reflections to travel from the walls of the tank to the contraction. Thus, the height amplitude formalism used by [Phu \(2001\)](#) to characterise tidal strength may be distorted by resonant effects.

It follows from this analysis that one can most easily describe geophysical observations using barotropic flux amplitude. However, measurements of tidal range are easiest to quantify in terms of height amplitude, rather than flux. It is likely that a barotropic model of the tidal velocities will be required to be able to apply [Helfrich's \(1995\)](#) formalism with any confidence.

Acknowledgements. J. Nycander contributed significantly to this work, in assisting with the implementation of the boundary conditions and commenting on early drafts of this manuscript. LMF was funded by an A. L. Hales Scholarship, and AMH acknowledges the support of an Australian Research Council Postdoctoral Fellowship (DP0449851). This work was supported by the National Facility of the Australian Partnership for Advanced Computing.

References

- Armi, L.: The hydraulics of two flowing layers with different densities, *J. Fluid Mech.*, 163, 27–58, 1986. [2000](#)
- Armi, L. and Farmer, D. M.: Maximal two-layer exchange through a contraction with barotropic net flow, *J. Fluid Mech.*, 164, 27–51, 1986. [2000](#), [2001](#), [2002](#)
- Armi, L. and Farmer, D. M.: A Generalization of the concept of Maximal Exchange in a Strait, *J. Geophys. Res.*, 92, 14 679–14 680, 1987. [2000](#)

Tides in exchange flows

L. M. Frankcombe and
A. McC. Hogg

Title Page

Abstract

Introduction

Conclusions

References

Tables

Figures

◀

▶

◀

▶

Back

Close

Full Screen / Esc

Printer-friendly Version

Interactive Discussion

- Bray, N., Ochoa, W. J., and Kinder, T.: The role of the interface in exchange through the Strait of Gibraltar, *J. Geophys. Res.*, 100, 10 755–10 776, 1995. [2000](#)
- Harvey, J. and Arhan, M.: The Water Masses of the Central North Atlantic in 1983-84, *J. Phys. Oceanogr.*, 18, 1855–1875, 1988. [2000](#)
- 5 Helfrich, K. L.: Time-dependent two-layer hydraulic exchange flow, *J. Phys. Oceanogr.*, 25, 359–373, 1995. [2000](#), [2001](#), [2002](#), [2007](#), [2008](#), [2009](#), [2010](#)
- Ivey, G. N.: Stratification and mixing in sea straits, *Deep-Sea Res. II*, 51, 441–453, 2004. [2001](#), [2010](#)
- Nycander, J. and Döös, K.: Open boundary conditions for barotropic waves, *J. Geophys. Res.*, 108, 10.1029/2002JC001 529, 2003. [2003](#)
- 10 Nycander, J., Hogg, A. M., and Frankcombe, L. M.: Open boundary conditions for nonlinear shallow water models, *Ocean Modell.*, p. Submitted for Review, 2006. [2003](#), [2006](#), [2008](#), [2012](#)
- Phu, A.: Tidally forced exchange flows, Honours thesis, University of Western Australia, 2001. [2001](#), [2002](#), [2008](#), [2009](#), [2010](#)
- 15 Stigebrandt, A.: On the effects of barotropic current fluctuations on the two-layer transport capacity of a constriction, *J. Phys. Oceanogr.*, 7, 118–122, 1977. [2000](#)
- Sy, A.: Investigation of large-scale circulation patterns in the Central North Atlantic: the North Atlantic Current, the Azores Current, and the Mediterranean Water plume in the area of the Mid-Atlantic Ridge, *Deep Sea Res.*, 35, 383–413, 1988. [2000](#)
- 20 Wood, I. R.: A lock exchange flow, *J. Fluid Mech.*, 42, 671–687, 1970. [2000](#)

Tides in exchange flows

L. M. Frankcombe and
A. McC. Hogg

[Title Page](#)[Abstract](#)[Introduction](#)[Conclusions](#)[References](#)[Tables](#)[Figures](#)[◀](#)[▶](#)[◀](#)[▶](#)[Back](#)[Close](#)[Full Screen / Esc](#)[Printer-friendly Version](#)[Interactive Discussion](#)

Tides in exchange flows

L. M. Frankcombe and
A. McC. Hogg

Title Page

Abstract

Introduction

Conclusions

References

Tables

Figures

◀

▶

◀

▶

Back

Close

Full Screen / Esc

Printer-friendly Version

Interactive Discussion

Table 1. Standard physical and computational parameters for simulations. See Nycander et al. (2006) for an explanation for the values of the internal and external characteristics.

Parameter	Value	Description
l	0.5 m	Constriction length
A_h	$0.008 \text{ m}^2/\text{s}$	Horizontal viscosity
H	0.4 m	Total fluid height
b_{\min}	0.1 m	Minimum channel width (at $x = 0$)
b_{\max}	0.2 m	Maximum channel width (at $x = \pm L$)
g'	0.1 m/s^2	Reduced gravity
L	0.5 m	Channel length
Δt	$3 \times 10^{-7} \text{ s}$	Timestep
n	201	Number of gridpoints
Δx	0.005 m	Gridlength
a_e^+	0.017	External BC coefficient at LHS
a_e^-	0.0	External BC coefficient at RHS
a_i^+	0.07028	Internal BC coefficient at LHS
a_i^-	-0.07028	Internal BC coefficient at RHS

Tides in exchange flows

L. M. Frankcombe and
A. McC. Hogg

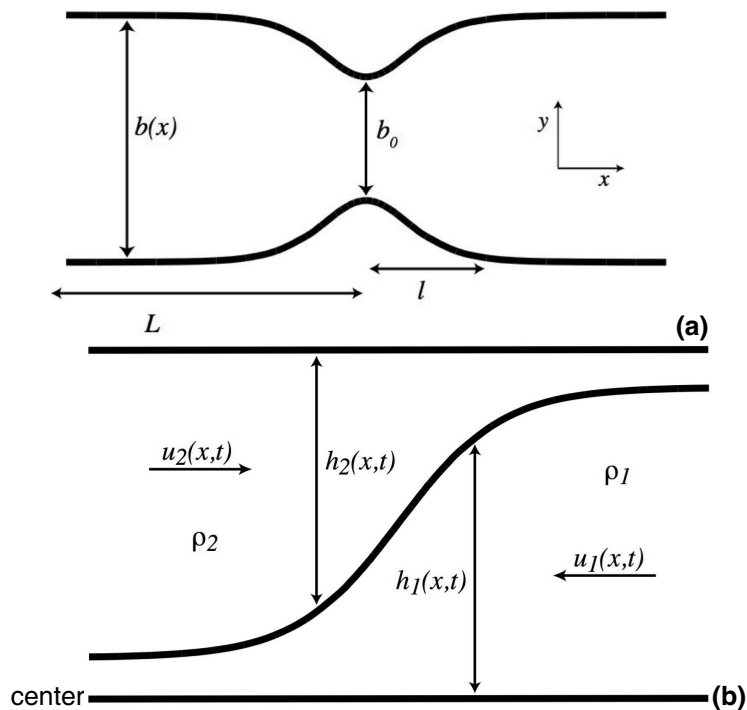


Fig. 1. Schematic showing (a) plan and (b) elevation view of the flow.

[Title Page](#)
[Abstract](#)
[Introduction](#)
[Conclusions](#)
[References](#)
[Tables](#)
[Figures](#)
[◀](#)
[▶](#)
[◀](#)
[▶](#)
[Back](#)
[Close](#)
[Full Screen / Esc](#)
[Printer-friendly Version](#)
[Interactive Discussion](#)

Tides in exchange flows

L. M. Frankcombe and
A. McC. Hogg

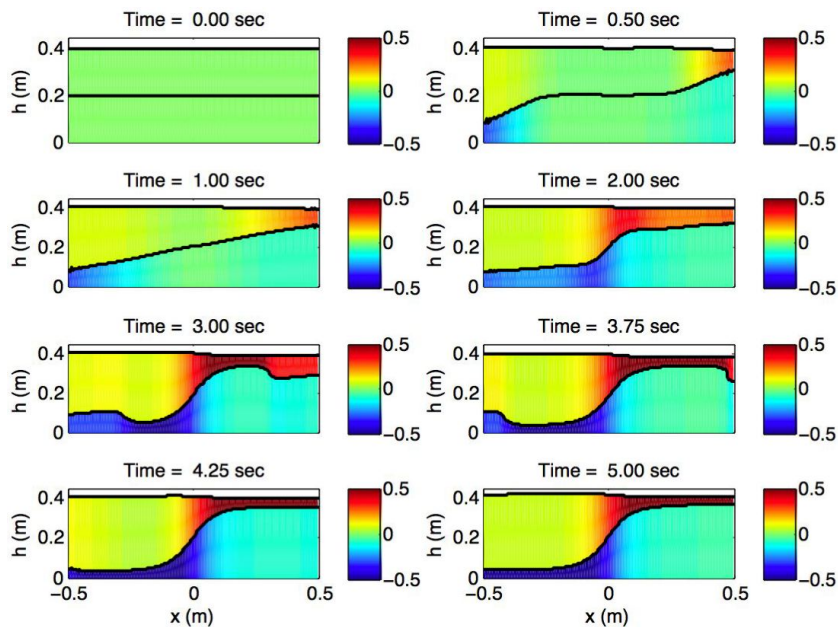
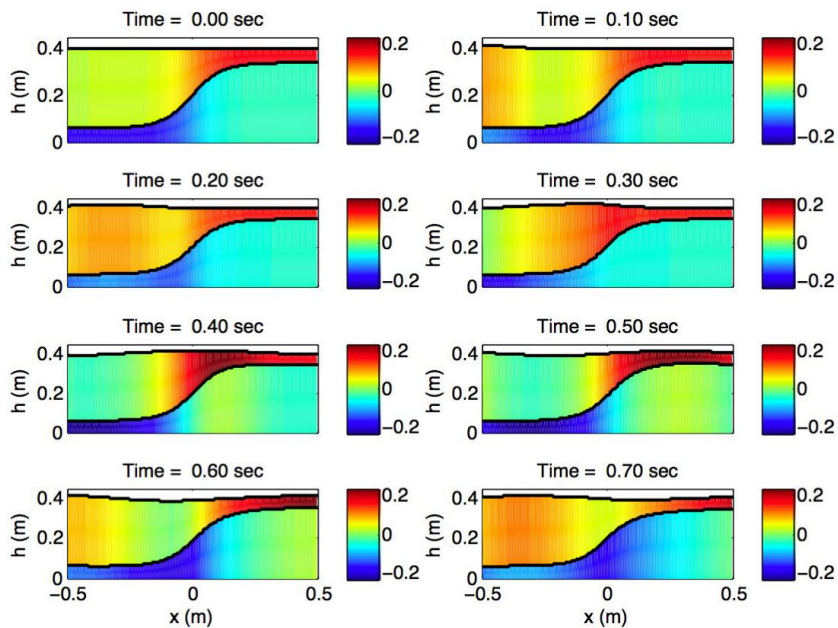


Fig. 2. Development of two layer flow (for a channel with $b_{\max}=0.3$ m).

[Title Page](#)
[Abstract](#)
[Introduction](#)
[Conclusions](#)
[References](#)
[Tables](#)
[Figures](#)
[⏪](#)
[⏩](#)
[◀](#)
[▶](#)
[Back](#)
[Close](#)
[Full Screen / Esc](#)
[Printer-friendly Version](#)
[Interactive Discussion](#)

Tides in exchange flowsL. M. Frankcombe and
A. McC. Hogg**Fig. 3.** Propagation of a wave through the channel.[Title Page](#)[Abstract](#)[Introduction](#)[Conclusions](#)[References](#)[Tables](#)[Figures](#)[◀](#)[▶](#)[◀](#)[▶](#)[Back](#)[Close](#)[Full Screen / Esc](#)[Printer-friendly Version](#)[Interactive Discussion](#)

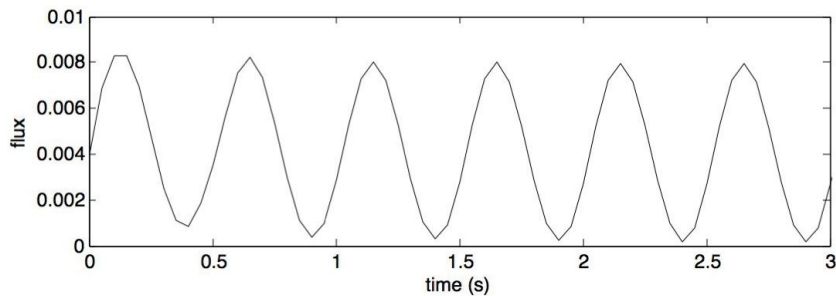
Tides in exchange flowsL. M. Frankcombe and
A. McC. Hogg

Fig. 4. Barotropic flux measured at the left hand boundary.

[Title Page](#)[Abstract](#)[Introduction](#)[Conclusions](#)[References](#)[Tables](#)[Figures](#)[◀](#)[▶](#)[◀](#)[▶](#)[Back](#)[Close](#)[Full Screen / Esc](#)[Printer-friendly Version](#)[Interactive Discussion](#)

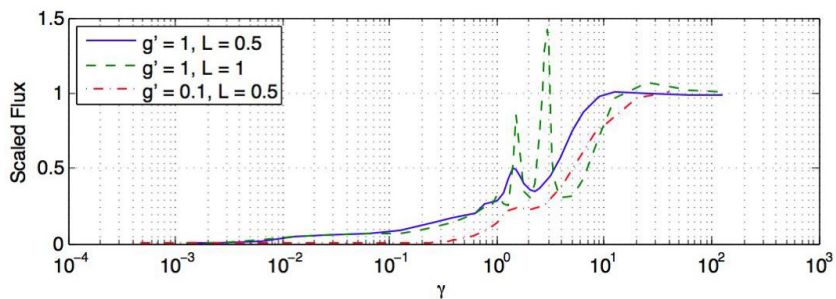
Tides in exchange flowsL. M. Frankcombe and
A. McC. Hogg

Fig. 5. Flux anomaly with different values of g' and L , scaled by the quasi-steady flux.

[Title Page](#)[Abstract](#)[Introduction](#)[Conclusions](#)[References](#)[Tables](#)[Figures](#)[◀](#)[▶](#)[◀](#)[▶](#)[Back](#)[Close](#)[Full Screen / Esc](#)[Printer-friendly Version](#)[Interactive Discussion](#)

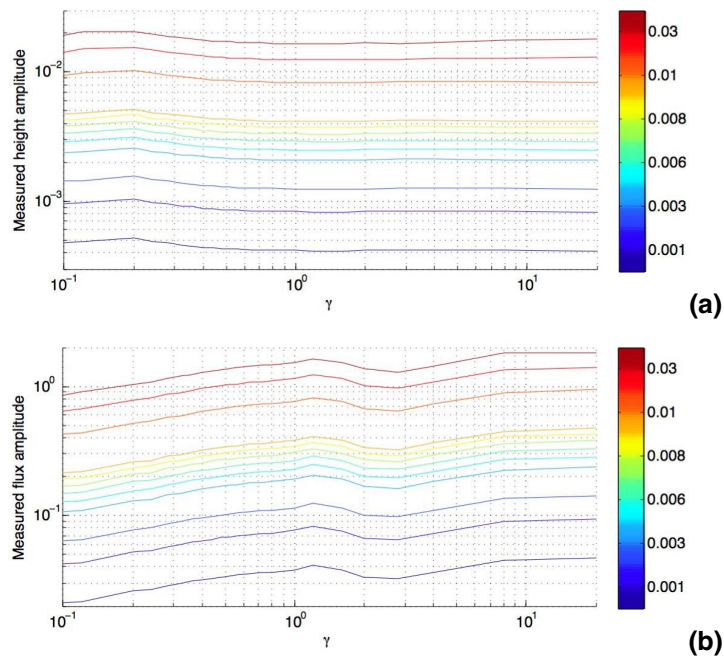
Tides in exchange flowsL. M. Frankcombe and
A. McC. Hogg

Fig. 6. Observed **(a)** height and **(b)** flux amplitudes are plotted against γ for different imposed a_e^+ amplitudes.

[Title Page](#)[Abstract](#)[Introduction](#)[Conclusions](#)[References](#)[Tables](#)[Figures](#)[◀](#)[▶](#)[◀](#)[▶](#)[Back](#)[Close](#)[Full Screen / Esc](#)[Printer-friendly Version](#)[Interactive Discussion](#)

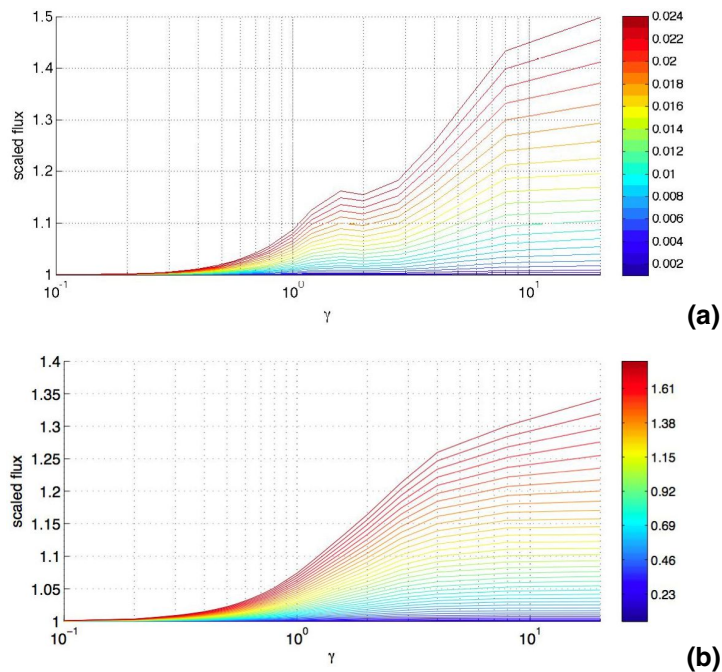
Tides in exchange flowsL. M. Frankcombe and
A. McC. Hogg

Fig. 7. Flux is plotted against γ with (a) measured height amplitude and (b) measured flux amplitude in colour.

[Title Page](#)[Abstract](#)[Introduction](#)[Conclusions](#)[References](#)[Tables](#)[Figures](#)[◀](#)[▶](#)[◀](#)[▶](#)[Back](#)[Close](#)[Full Screen / Esc](#)[Printer-friendly Version](#)[Interactive Discussion](#)

Tides in exchange flows

L. M. Frankcombe and
A. McC. Hogg

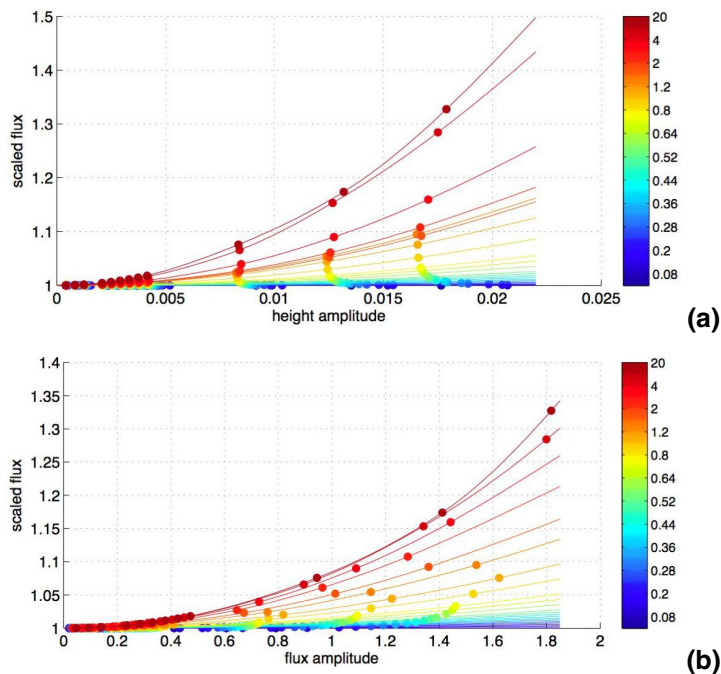


Fig. 8. Flux is plotted against (a) measured height amplitude and (b) measured flux amplitude, with γ in colour. Solid circles show the original points from which the other points have been interpolated.

[Title Page](#)
[Abstract](#)
[Introduction](#)
[Conclusions](#)
[References](#)
[Tables](#)
[Figures](#)
[◀](#)
[▶](#)
[◀](#)
[▶](#)
[Back](#)
[Close](#)
[Full Screen / Esc](#)
[Printer-friendly Version](#)
[Interactive Discussion](#)